

# Supplementary Material for “RGB-Infrared Cross-Modality Person Re-Identification”

Ancong Wu, Wei-Shi Zheng, Hong-Xing Yu, Shaogang Gong and Jianhuang Lai

## Abstract

*This supplementary material accompanies the paper “RGB-Infrared Cross-Modality Person Re-Identification”. It includes more details of Section 4, as well as extra evaluations of our proposed deep zero-padding method.*

## 1. Details of Counting Domain-Specific Nodes

In the third paragraph of Section 4.2 in the main manuscript, we quantify the number of domain-specific nodes in the trained network in our experiments.

As defined in Equation (3) in Section 3 in the main manuscript, the categorization of node types is rather strict. In the  $l$ -th layer, let  $\eta_i^{(l)}$  denote the  $i$ -th node and  $f_{out}(\mathbf{x}^{(0)}, i, l)$  denote the output of  $\eta_i^{(l)}$  given the network input  $\mathbf{x}^{(0)}$ . Let  $\mathbf{x}_{d1}^{(0)}$  and  $\mathbf{x}_{d2}^{(0)}$  be inputs of the whole network of domain1 and domain2, respectively. The type of node  $\eta_i^{(l)}$  is defined by

$$type(\eta_i^{(l)}) = \begin{cases} domain1 - specific, & f_{out}(\mathbf{x}_{d2}^{(0)}, i, l) \equiv 0 \\ domain2 - specific, & f_{out}(\mathbf{x}_{d1}^{(0)}, i, l) \equiv 0 \\ shared, & otherwise. \end{cases} \quad (1)$$

Since the identity sign is used here, the categorization condition is too strict in applications. So we relax the categorization condition for counting towards domain-specific nodes in application by setting a threshold  $T$ . The relaxed definition of node type is formulated as follows: for all  $\mathbf{x}_{d1}^{(0)}$  and  $\mathbf{x}_{d2}^{(0)}$  in our experiments,

$$type(\eta_i^{(l)}) = \begin{cases} domain1 - specific, & f_{out}(\mathbf{x}_{d2}^{(0)}, i, l) < T \text{ and} \\ & f_{out}(\mathbf{x}_{d1}^{(0)}, i, l) > T \\ domain2 - specific, & f_{out}(\mathbf{x}_{d1}^{(0)}, i, l) < T \text{ and} \\ & f_{out}(\mathbf{x}_{d2}^{(0)}, i, l) > T \\ shared, & otherwise. \end{cases} \quad (2)$$

Because the scales of responses on feature maps differ from layer to layer, we set  $T = \alpha \text{std}(x_i^{(l)})$ , where  $\alpha$  is a proportion coefficient,  $x_i^{(l)}$  is the output value of the  $i$ -th node

in the  $l$ -th layer and  $\text{std}(\cdot)$  is the standard deviation function. For an image channel in our experiments, we compute the average of all values in the feature map as the output of the node. We set  $\alpha = 0.01$  and  $\alpha = 0.05$  for strict and loose categorizations, respectively. The relation between the proportion of domain-specific nodes and layer depth is shown in Figure S1. Both total proportions and respective proportions of two domains are shown. With strict threshold, domain-specific nodes mainly exist in the first three layers. With loose threshold, domain-specific nodes mainly exist in the first five layers. In both cases, the network can learn more domain-specific nodes using deep zero-padding. When the threshold is loosened, the proportion of domain-specific nodes increases when using deep zero-padding, but keeps nearly unchanged when using the inputs without zero-padding.

## 2. Evaluation on Using Different Networks

Our deep model is based on ResNet [1] as illustrated in Section 5 in the main manuscript. Deep zero-padding has shown effectiveness on ResNet-6 in our experiments. To verify whether deep zero-padding can also work with other one-stream networks, we also evaluated our method on popular architectures AlexNet [2] and VGG-16 [3]. The results are reported in Table S1.

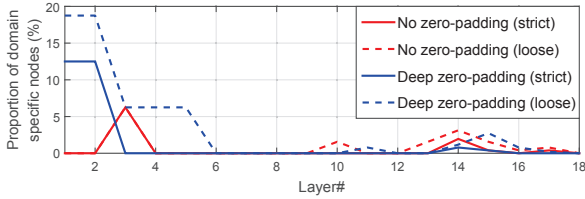
Generally, using deep zero-padding can improve the performance in most cases for all evaluated network architectures. The improvement is especially evident for ResNet-6.

## References

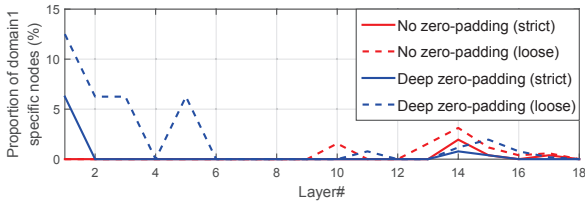
- [1] K. He, X. Zhang, S. Ren, and J. Sun. Deep residual learning for image recognition. In *CVPR*, 2016. 1
- [2] A. Krizhevsky, I. Sutskever, and G. E. Hinton. Imagenet classification with deep convolutional neural networks. In *NIPS*, 2012. 1
- [3] K. Simonyan and A. Zisserman. Very deep convolutional networks for large-scale image recognition. In *ICLR*, 2015. 1

Table S1. Performance under all-search and indoor-search using different networks, where r1, r10, r20 denote rank-1, 10, 20 accuracies (%), respectively and mAP denotes mean average precision (%).

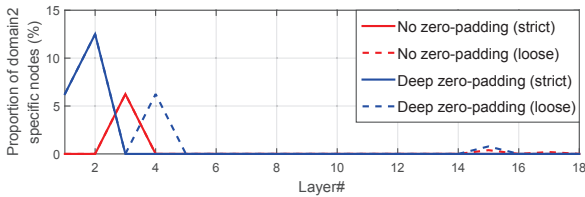
Method	Metric	All-search								Indoor-search							
		Single-shot				Multi-shot				Single-shot				Multi-shot			
		r1	r10	r20	mAP	r1	r10	r20	mAP	r1	r10	r20	mAP	r1	r10	r20	mAP
ResNet-6 (deep zero-padding)	Euclidean	<b>14.80</b>	<b>54.12</b>	<b>71.33</b>	<b>15.95</b>	<b>19.13</b>	<b>61.40</b>	<b>78.41</b>	<b>10.89</b>	<b>20.58</b>	<b>68.38</b>	<b>85.79</b>	<b>26.92</b>	<b>24.43</b>	<b>75.86</b>	<b>91.32</b>	<b>18.64</b>
ResNet-6	Euclidean	12.04	49.68	66.74	13.67	16.26	58.14	75.05	8.59	16.94	63.55	82.10	22.95	22.62	71.74	87.82	15.04
VGG-16 (deep zero-padding)	Euclidean	<b>9.23</b>	<b>39.14</b>	<b>55.38</b>	<b>9.60</b>	<b>11.45</b>	<b>45.50</b>	<b>62.41</b>	<b>5.93</b>	<b>11.45</b>	<b>53.18</b>	<b>73.73</b>	<b>17.20</b>	<b>14.82</b>	<b>62.01</b>	<b>80.88</b>	<b>10.13</b>
VGG-16	Euclidean	7.46	36.52	51.71	8.69	9.42	43.49	60.30	5.20	10.61	50.02	70.29	16.25	14.27	60.97	79.87	9.37
AlexNet (deep zero-padding)	Euclidean	<b>9.70</b>	<b>43.14</b>	<b>59.25</b>	<b>11.00</b>	<b>11.52</b>	<b>50.04</b>	<b>67.50</b>	<b>6.68</b>	<b>12.96</b>	<b>55.88</b>	75.45	<b>19.12</b>	15.41	<b>62.51</b>	<b>81.22</b>	<b>11.71</b>
AlexNet	Euclidean	9.48	41.63	57.96	10.32	11.07	49.38	66.53	6.21	12.69	55.40	<b>75.50</b>	18.67	<b>16.16</b>	61.31	79.73	11.42



(a) Proportions of domain-specific nodes



(b) Proportions of domain1-specific (RGB) nodes



(c) Proportions of domain2-specific (IR) nodes

Figure S1. Relation between proportion of domain-specific nodes and layer depth. The x-axis denotes layer depth from bottom to top of the network, and the y-axis denotes the proportion of domain-specific nodes. Generally, the proportion of domain-specific nodes using deep zero-padding is higher than that without zero-padding.